*J. Fluid Mech.* (2016), *vol.* 794, *pp.* 233–251. © Cambridge University Press 2016
doi:10.1017/jfm.2016.172



# Generalised higher-order Kolmogorov scales

**Jonas Boschung[1,†], Fabian Hennig[1], Michael Gauding[2], Heinz Pitsch[1] and Norbert Peters[1]**

[1]Institute for Combustion Technology, RWTH Aachen University, Templergraben 64, Aachen, Germany

[2]Chair of Numerical Thermo-Fluid Dynamics, TU Bergakademie, Fuchsmühlenweg 9, Freiberg, Germany

(Received 9 November 2015; revised 25 February 2016; accepted 29 February 2016;
first published online 30 March 2016)

Kolmogorov introduced dissipative scales based on the mean dissipation $\langle\varepsilon\rangle$ and the viscosity $\nu$, namely the Kolmogorov length $\eta = (\nu^3/\langle\varepsilon\rangle)^{1/4}$ and the velocity $u_\eta = (\nu\langle\varepsilon\rangle)^{1/4}$. However, the existence of smaller scales has been discussed in the literature based on phenomenological intermittency models. Here, we introduce exact dissipative scales for the even-order longitudinal structure functions. The derivation is based on exact relations between even-order moments of the longitudinal velocity gradient $(\partial u_1/\partial x_1)^{2m}$ and the dissipation $\langle\varepsilon^m\rangle$. We then find a new length scale $\eta_{C,m} = (\nu^3/\langle\varepsilon^{m/2}\rangle^{2/m})^{1/4}$ and $u_{C,m} = (\nu\langle\varepsilon^{m/2}\rangle^{2/m})^{1/4}$, i.e. the dissipative scales depend rather on the moments of the dissipation $\langle\varepsilon^{m/2}\rangle$ and thus the full probability density function (p.d.f.) $P(\varepsilon)$ instead of powers of the mean $\langle\varepsilon\rangle^{m/2}$. The results presented here are exact for longitudinal even-ordered structure functions under the assumptions of (local) isotropy, (local) homogeneity and incompressibility, and we find them to hold empirically also for the mixed and transverse as well as odd orders. We use direct numerical simulations (DNS) with Reynolds numbers from $Re_\lambda = 88$ up to $Re_\lambda = 754$ to compare the different scalings. We find that indeed $P(\varepsilon)$ or, more precisely, the scaling of $\langle\varepsilon^{m/2}\rangle/\langle\varepsilon\rangle^{m/2}$ as a function of the Reynolds number is a key parameter, as it determines the ratio $\eta_{C,m}/\eta$ as well as the scaling of the moments of the velocity gradient p.d.f. As $\eta_{C,m}$ is smaller than $\eta$, this leads to a modification of the estimate of grid points required for DNS.

**Key words:** isotropic turbulence, turbulent flows

## 1. Introduction

Kolmogorov (1941*b*) introduced the idea of local isotropy, i.e. that turbulence is isotropic at small scales (and possibly universally), provided that the Reynolds number is large enough so that a scale separation occurs, while the large scales are determined by the flow geometry and boundary conditions. Furthermore, Kolmogorov proposed two similarity laws. The first similarity hypothesis states that, for locally homogeneous and isotropic turbulence, the statistics of structure functions, defined as the velocity difference between two points separated by a distance $r$, are determined by the viscosity $\nu$ and the mean dissipation $\langle\varepsilon\rangle$. For $r$ situated in the inertial range between the very small scales and the large scales, the dependence on the viscosity

† Email address for correspondence: j.boschung@itv.rwth-aachen.de

$\nu$ should vanish according to the second hypothesis of similarity. From the two quantities $\nu$ and $\langle\varepsilon\rangle$ relevant at the very small scales, he introduced $\eta = (\nu^3/\langle\varepsilon\rangle)^{1/4}$ and $u_\eta = (\nu/\langle\varepsilon\rangle)^{1/2}$ as characteristic length and velocity scales, which were derived for the second order. The main focus of the present work is to revisit these results and generalise them for higher orders under the same assumptions, i.e. (local) isotropy, (local) homogeneity and incompressibility. We are able to present some new and exact results for longitudinal, even-ordered structure functions.

In a second paper, Kolmogorov (1941*a*) proceeded to rewrite the Kármán–Howarth equation (cf. de Karman & Howarth 1938) in terms of the second-order longitudinal structure function. This led to analytic solutions for the second-order structure function for $r \to 0$, which agrees with his previously derived result using only isotropy and Taylor series, as given in the first 1941 paper, and the third-order structure function in the inertial range $\eta \ll r \ll L$ under the assumption of very large (infinite) Reynolds number, where $L$ is the integral length scale.

The two papers had a huge impact, as they provided specific predictions about the nature of turbulent flows stemming directly from the governing Navier–Stokes equations, one of which is that in the inertial range the structure functions should follow a power law in terms of the separation distance $r$. Furthermore, Kolmogorov's postulate that velocity differences at small scales are isotropic, leading to the idea that some small-scale properties should be flow-independent, is quite appealing (see Sreenivasan & Antonia (1997) for an overview). It was found that, although Kolmogorov's results for the second- and third-order structure functions are in very good agreement with measurements (see e.g. Anselmet, Gagne & Hopfinger 1984), the generalisation to higher orders is rather poor. For instance, the experimentally observed inertial range power-law exponents $\zeta_m$ at higher orders deviate significantly from the values one would obtain by applying Kolmogorov's original postulate that only the mean dissipation $\langle\varepsilon\rangle$ and $\nu$ are relevant. For that matter, Kolmogorov (1962) modified his theory following Obukhov (1962) based on the phenomenological observation that turbulent fluctuations of the dissipation play a crucial role in turbulence. In particular, they substituted a locally averaged dissipation $\varepsilon_r$ for the overall dissipation $\langle\varepsilon\rangle$ and assumed a log-normal distribution for $\varepsilon_r$. This led the way to (multi-)fractal models providing equations for $\zeta_m$ using some additional parameters (see Sreenivasan (1991) and Frisch (1995) for overviews). Equations for structure functions of all orders were derived by Hill (2001) and Yakhot (2001), using different methods.

The notion of order-dependent cut-off length scales is also related to the multi-fractal framework – see, for example, Paladin & Vulpiani (1987*a*,*b*), who used the multi-fractal model to estimate grid resolution scaling. Frisch & Vergassola (1991) used the notion of scales smaller than the Kolmogorov scale to modify the second-order structure function as well as the energy spectrum in the so-called intermediate dissipation range (situated in between the Kolmogorov scale and the smallest scale determined by the lowest fractal exponent). They then proposed a renormalisation of the energy spectrum to collapse it to a universal curve.

Meneveau (1996) examined the dissipative range by employing an order-dependent interpolation formula accompanied by using a multi-fractal model to examine order- and Reynolds-number-dependent collapse of structure functions in the dissipative range. He showed that order-dependent cut-off length scales as given by a multi-fractal model are consistent with extended self-similarity (ESS; cf. Benzi *et al.* 1993) for small Reynolds numbers, but that the collapse of ESS worsens for high Reynolds numbers and order.

Yakhot (2003) derived order-dependent cut-off length scales by matching the dissipative range and the inertial range, and related these cut-off scales to the inertial range exponents $\zeta_m$. Yakhot & Sreenivasan (2005) then used Yakhot's result and derived additional constraints on the inertial range scaling exponents. Furthermore, they considered the implications regarding the grid resolution of numerical studies in the context of Yakhot's theory. More recently, Schumacher, Sreenivasan & Yakhot (2007) examined structure functions using highly resolved direct numerical simulations (DNS) and found that they collapse in the dissipation range when normalised with the cut-off lengths defined by the inertial range exponents given by Yakhot (2003).

The approach presented in this paper differs from those described above inasmuch as we derive cut-off scales by using information gained from the (isotropic) tensorial properties of the velocity gradient tensor, for which we do not need any specific assumptions other than isotropy, homogeneity and incompressibility. This allows us to define the cut-off scales with dissipative quantities only (namely, the moments of the dissipation), and we find exact relations for the longitudinal structure functions of arbitrary even order, using only the same assumptions as in Kolmogorov's seminal 1941 work (henceforth often abbreviated as K41).

The paper is organised as follows. We use data from DNS, which are described in § 2. In § 3, we look at velocity structure functions in the dissipative range and find analytical relations for even-order longitudinal structure functions. From these follow new $m$th-order cut-off length scales $\eta_{C,m}$ and velocities $u_{C,m}$, resulting in Reynolds-number-independent non-dimensional structure functions in the dissipation range, which we discuss and check against our DNS data. We want to emphasise that these results are not connected in any way to the multi-fractal models, in the sense that those models are not needed to derive the results presented here. However, any theory predicting the scaling of the dissipation $\varepsilon_r$ predicts the scaling of the normalised moments of the dissipation in the dissipative range and therefore also of $\eta_{C,m}$. This is examined in detail in § 4, and we compare the results obtained from some well-known models to our DNS. The new scales $\eta_{C,m}$ and $u_{C,m}$ lead to modifications of grid resolution requirements for DNS and to a modified scaling of the number of grid points as discussed in § 5. Different from previous studies (e.g. Yakhot & Sreenivasan 2005), we use the exact results of § 3 instead of those stemming from multi-fractal models. We then summarise the results in § 6.

## 2. Direct numerical simulations

For the analysis carried out in the present paper, we use data from DNS of forced homogeneous isotropic turbulence with six different sets of Taylor-based Reynolds numbers, ranging from $Re_\lambda = 88$ to $Re_\lambda = 754$, where $Re_\lambda = u_{rms}\lambda/\nu$, $\lambda$ denotes the Taylor scale $\lambda = \sqrt{10\nu\langle k\rangle/\langle\varepsilon\rangle}$, $u_{rms} = \langle u_i u_i/3\rangle$ is the root-mean-square velocity, $\langle k\rangle = \langle u_i u_i\rangle/2$ is the mean kinetic energy and $\langle\varepsilon\rangle = 2\nu\langle S_{ij}S_{ij}\rangle$ is the mean energy dissipation, with the strain tensor $S_{ij} = (\partial u_i/\partial x_j + \partial u_j/\partial x_i)/2$. Angle brackets $\langle\cdots\rangle$ denote ensemble averages over the full box and several time steps spanning more than an integral turnover time after the simulation has reached its statistically steady state (as given by the ratio $t_{avg}/\tau$). We use $M$ to denote the number of time steps used to compute the averages.

The six datasets have been computed on the JUQUEEN supercomputer at Forschungszentrum Jülich using a pseudo-spectral code with MPI/OpenMP parallelisation. The three-dimensional Navier–Stokes equations were solved in rotational form, where all terms except the nonlinear term were evaluated in spectral space.

| | R0 | R1 | R2 | R3 | R4 | R5 |
|---|---|---|---|---|---|---|
| $N$ | 512 | 1024 | 1024 | 2048 | 2048 | 4096 |
| $Re_\lambda$ | 88 | 119 | 184 | 215 | 331 | 754 |
| $\nu$ | 0.01 | 0.0055 | 0.0025 | 0.0019 | 0.0010 | 0.00027 |
| $\kappa_{max}\eta$ | 3.57 | 4.54 | 2.66 | 4.01 | 2.30 | 1.76 |
| $\langle k \rangle$ | 11.15 | 11.38 | 11.42 | 12.70 | 14.35 | 24.42 |
| $\langle \varepsilon \rangle$ | 10.78 | 11.04 | 10.30 | 11.87 | 12.55 | 26.54 |
| $\lambda$ | 0.322 | 0.238 | 0.166 | 0.143 | 0.107 | 0.050 |
| $\eta$ | 0.0175 | 0.0111 | 0.0062 | 0.0049 | 0.0030 | 0.00093 |
| $L$ | 1.02 | 0.94 | 0.97 | 1.01 | 0.97 | 1.18 |
| $\tau_\eta$ | 0.031 | 0.022 | 0.016 | 0.013 | 0.009 | 0.0032 |
| $\tau$ | 1.03 | 1.03 | 1.11 | 1.07 | 1.14 | 0.92 |
| $t_{avg}/\tau$ | 100 | 30 | 30 | 10 | 10 | 3 |
| $M$ | 112 | 42 | 40 | 10 | 10 | 6 |

TABLE 1. Characteristics of DNS cases.

For a faster computation, the nonlinear term is evaluated in physical space. The computational domain is a box with periodic boundary conditions and length $2\pi$. For dealiasing, the scheme of Hou & Li (2007) has been used. For the temporal advancement, a second-order Adams–Bashforth scheme is used in the case of the nonlinear term, while the linear terms are updated using a Crank–Nicolson scheme. To keep the simulation statistically steady, the stochastic forcing scheme of Eswaran & Pope (1988) is applied. The 2DECOMP and FFT library (Li & Laizet 2010) has been used for spatial decomposition and to perform the fast Fourier transforms. The only parameter varied to increase the Reynolds number is the viscosity $\nu$; the forcing parameters have been held constant. The properties of the DNS cases can be found in table 1. The five datasets were computed on a computational mesh with $512^3$ grid points for case R0 up to $4096^3$ grid points for case R5. There, $\eta = (\nu^3/\langle\varepsilon\rangle)^{1/4}$ is the Kolmogorov length scale with corresponding time scale $\tau_\eta = (\nu/\langle\varepsilon\rangle)^{1/2}$, $L$ is the integral length scale, computed here using the energy spectrum function

$$L = \frac{3\pi}{4}\frac{\int \kappa^{-1}E(\kappa)\,\mathrm{d}\kappa}{\int E(\kappa)\,\mathrm{d}\kappa}, \tag{2.1}$$

and $\tau = \langle k\rangle/\langle\varepsilon\rangle$ is the integral time scale. The integral length scale $L$ is small compared to the size of the boxes in order to reduce the influence of the periodic boundary condition. Our data are well resolved with $\kappa_{max}\eta \geqslant 1.7$ for all five datasets, where $\kappa_{max}$ is the largest resolved wavenumber. In turn, this also implies that the Reynolds number is not as high as for other DNS with comparable mesh size reported in the literature. We discuss this in more detail in § 5.

## 3. Dissipative cut-off scales

Kolmogorov's first similarity hypothesis (cf. Kolmogorov 1941*b*) states that 'for the locally isotropic turbulence the distributions $F_n$ are uniquely determined by the

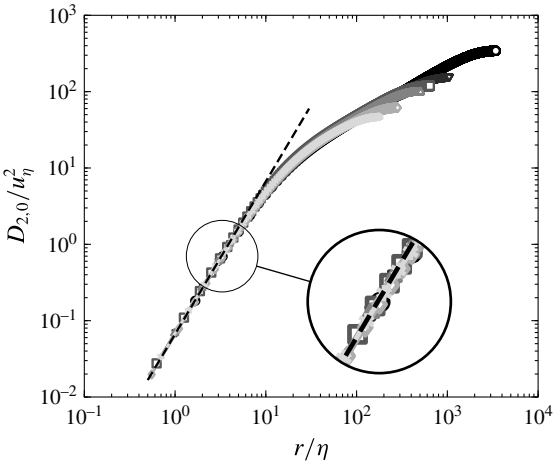


FIGURE 1. Longitudinal structure function $D_{20}$ normalised with $\eta$ and $u_\eta$ for: $*$, $Re_\lambda = 88$; $\diamond$, $Re_\lambda = 119$; $\triangle$, $Re_\lambda = 184$; $\square$, $Re_\lambda = 215$; $\triangledown$, $Re_\lambda = 331$; and $\bigcirc$, $Re_\lambda = 754$. The dashed line corresponds to (3.16) with $\widetilde{K}_{2,0} = 1/15$.

quantities $\nu$ and $\langle\varepsilon\rangle$', where $F_n$ are the distributions of the velocity increments (note that Frisch (1995) interprets $F_n$ as 'small-scale properties'). In other words, all structure functions $D_{p,q} = \langle[\Delta u_1]^p[\Delta u_2]^q\rangle$ (where $\Delta u_j = u_j(\boldsymbol{x}_i + \boldsymbol{r}_i) - u_j(\boldsymbol{x}_i)$ and the separation vector $\boldsymbol{r}_i$ with magnitude $r$ is aligned without loss of generality with the $x_1$ axis) are supposed to be uniquely determined by the viscosity $\nu$ and the mean dissipation $\langle\varepsilon\rangle$ for $r \to 0$. Kolmogorov backed up this claim by determining the solution for the second-order structure functions in the dissipative range,

$$D_{2,0} = \frac{1}{2}D_{0,2} = \frac{1}{15}\frac{\langle\varepsilon\rangle}{\nu}r^2, \tag{3.1}$$

where he obtained the factor 15 by relating the mean dissipation $\langle\varepsilon\rangle$ to $\langle(\partial u_1/\partial x_1)^2\rangle$ (Kolmogorov 1941*b*). Indeed, it is possible to express the full tensor $\langle(\partial u_i/\partial x_j)(\partial u_k/\partial x_l)\rangle$ by a single scalar (e.g. the mean dissipation) under the assumption of isotropy, homogeneity and incompressibility, which implies that $D_{2,0}$ and $D_{0,2}$ are exactly related in the dissipative range. Figure 1 shows the second-order structure function $D_{2,0}$ normalised in this way for the different Reynolds numbers given in § 2, which we show here to allow a visual comparison with higher-order structure functions normalised with the Kolmogorov scales $\eta$ and $u_\eta$ as presented below. In that spirit, the 'goodness of collapse' of the different curves onto a single curve as seen in figure 1 can be used as reference for the collapse or non-collapse of higher orders. We find that $D_{2,0}$ collapses indeed as expected and scales as $r^2$ for $r \to 0$. The dissipative range extends to $r/\eta \sim 10$ and is followed by a transitional region. For larger $r/\eta$, there is the inertial range which increases with increasing Reynolds number, in agreement with the classical picture of turbulent flows.

Generalising Kolmogorov's first similarity hypothesis implies

$$D_{m,0} = K_{m,0}\frac{\langle\varepsilon\rangle^{m/2}}{\nu^{m/2}}r^m, \tag{3.2}$$

where the constant $K_{m,0}$ should depend on the order $m$ only and is supposed to be independent of the Reynolds number. Non-dimensionalising this relation with the Kolmogorov velocity $u_\eta = (\nu\langle\varepsilon\rangle)^{1/4}$ and the Kolmogorov length $\eta = (\nu^3/\langle\varepsilon\rangle)^{1/4}$ gives

$$\frac{D_{m,0}}{u_\eta^m} = K_{m,0}\left(\frac{r}{\eta}\right)^m. \tag{3.3}$$

This implies that the structure functions should collapse for small $r \to 0$ according to (3.3) if normalised with $u_\eta$ and $\eta$. Taylor-expanding the structure functions of arbitrary order $m = p + q$, one finds

$$D_{p,q} = \left\langle \left(\frac{\partial u_1}{\partial x_1}\right)^p \left(\frac{\partial u_2}{\partial x_1}\right)^q \right\rangle r^{p+q} + \cdots. \tag{3.4}$$

In the following, we focus on longitudinal structure functions, for which there are exact results as presented below. We then have for $r \to 0$

$$D_{m,0} = \left\langle \left(\frac{\partial u_1}{\partial x_1}\right)^m \right\rangle r^m. \tag{3.5}$$

Similarly to Kolmogorov's approach for the second order, we then relate the moments of the longitudinal velocity gradient to the moments of the dissipation. One would immediately estimate that

$$\left\langle \left(\frac{\partial u_1}{\partial x_1}\right)^m \right\rangle \sim \frac{\langle\varepsilon^{m/2}\rangle}{\nu^{m/2}}, \tag{3.6}$$

i.e.

$$\left\langle \left(\frac{\partial u_1}{\partial x_1}\right)^m \right\rangle = \frac{\langle(S_{ij}S_{ij})^{m/2}\rangle}{C_{m,0}}, \tag{3.7}$$

in disagreement with Kolmogorov's first similarity hypothesis and (3.2), as the exponent and the averaging operator do not commute. The question then becomes whether $C_{m,0}$ is Reynolds-number-independent. For even $m$, it is possible to find the exact values of $C_{m,0}$ following Siggia (1981), as carried out by Boschung (2015). From this, we have $C_2 = 15/2$ (cf. (3.1)), $C_{4,0} = 105/4$ (cf. Siggia 1981), $C_{6,0} = 567/8$, $C_{8,0} = 2673/16$ and so on, and in general (for $m$ even)

$$C_{m,0} = \frac{3^{m/2-1}(m+1)(m+3)}{2^{m/2}}. \tag{3.8}$$

Consequently, for even $m$ we have

$$D_{m,0} = \widetilde{K}_{m,0}\frac{\langle\varepsilon^{m/2}\rangle}{\nu^{m/2}}r^m, \tag{3.9}$$

with $\widetilde{K}_{m,0} = (2^{m/2}C_{m,0})^{-1}$ and where the $C_{m,0}$ are exact, Reynolds-number-independent values as given by (3.8). Therefore, the even longitudinal structure function of order $m$ is determined by the moment $\langle\varepsilon^{m/2}\rangle$ of the dissipation and the viscosity $\nu$ for $r \to 0$ and we also have the exact solutions of some of the structure function equations for $r \to 0$ as the prefactor $C_{m,0}$ is also known. In other words, we have found the exact solution for arbitrary even-order structure functions in the dissipative range

analogously to Kolmogorov's result at the second order. Note that it is not possible to arrive at these conclusions simply on dimensional grounds, because $\langle \varepsilon^m \rangle$ and $\langle \varepsilon \rangle^m$ have the same dimensions.

What about the mixed and transverse structure functions at even orders? We note that these structure functions are not uniquely determined this way except for the second order $m = 2$, because the mixed derivatives $\langle (\partial u_1/\partial x_1)^p (\partial u_2/\partial x_1)^q \rangle$ are not completely determined by $\langle \varepsilon^{(p+q)/2} \rangle$. In other words, the higher-order tensors are not determined by only a single scalar function under the constraints of homogeneity and incompressibility. For instance, the general eighth-order velocity gradient tensor is determined by the four invariants $I_1$, $I_2$, $I_3$ and $I_4$ given by Siggia (1981) (cf. also Hierro & Dopazo 2003). In particular,

$$\left\langle \left( \frac{\partial u_1}{\partial x_1} \right)^4 \right\rangle = \frac{4}{105} I_1 = \frac{4}{105} \langle S_{ij} S_{ji} S_{kl} S_{lk} \rangle = \frac{1}{105} \frac{\langle \varepsilon^2 \rangle}{\nu^2}, \tag{3.10}$$

$$\left\langle \left( \frac{\partial u_1}{\partial x_1} \right)^2 \left( \frac{\partial u_2}{\partial x_1} \right)^2 \right\rangle = \frac{1}{105} I_1 + \frac{1}{70} I_2 - \frac{1}{105} I_3, \tag{3.11}$$

$$\left\langle \left( \frac{\partial u_2}{\partial x_1} \right)^4 \right\rangle = \frac{3}{140} I_1 + \frac{11}{140} I_2 - \frac{3}{35} I_3 + \frac{1}{80} I_4. \tag{3.12}$$

The invariants $I_1$, $I_2$, $I_3$ and $I_4$ are independent and therefore there are no relations between $I_1, \ldots, I_4$ and similarly at higher orders; consequently, the fourth-order mixed and transverse structure functions depend also on $I_2$, $I_3$ and $I_4$ and not solely on $I_1 \sim \langle \varepsilon^2 \rangle / \nu^2$. However, Ishihara *et al.* (2007) found that the ratios $I_2/I_1$, $I_3/I_1$ and $I_4/I_1$ are constant if the Reynolds number is large enough. This implies that all fourth-order structure functions scale with $\langle \varepsilon^2 \rangle$ for $r \to 0$ with universal prefactors including the mixed and transverse structure functions, although their prefactors cannot be determined analytically as multiples of the longitudinal prefactor, and the same holds at higher orders. Furthermore, the present approach cannot relate odd moments of the velocity gradients to moments of the dissipation. For the third order, we have the exact result $\langle (\partial u_1/\partial x_1)^3 \rangle = -2 \langle \omega_i S_{ij} \omega_j \rangle / 35$, which can be derived from the general sixth-order velocity gradient tensor (see Pope 2000) and which leads to the well-known relation between vortex stretching and the negative skewness of the velocity gradient (cf. e.g. Townsend 1951; Betchov 1956; Rotta 1972). As we have seen that the even longitudinal orders are determined by the moments of the dissipation, we will try to use $\langle \varepsilon^{3/2} \rangle$ and its generalisation, i.e. we will assume (3.9) to hold also for odd orders (albeit with unknown, but Reynolds-number-independent, $\widetilde{K}_{m,0}$). The only justification for odd orders up to this point is that this equation has the correct dimensions. Rather, we would expect the odd orders to scale with $\langle \omega_i S_{ij} S_{jk} \cdots \omega_l \rangle$, as these terms can be given in terms of the general velocity gradient tensor while terms like $\langle \varepsilon^{3/2} \rangle$ cannot.

We show higher even orders $D_{4,0}$, $D_{6,0}$ and $D_{8,0}$ normalised by $u_\eta$ and $\eta$ in the left column of figure 2 for different Reynolds numbers. Noticeably, these higher orders do not collapse and the disparity increases with Reynolds number and order $m$. This was anticipated by Landau & Lifshitz (1959) (cf. also Frisch 1995), who argued that $\langle \varepsilon \rangle$ could not be the relevant quantity for all orders $m$, i.e. that the proportionality factor $K_{m,0}$ of (3.3) should be flow-dependent. Normalising (3.9), K41 scaling then implies

$$\frac{D_{m,0}}{u_\eta^m} = \widetilde{K}_{m,0} \frac{\langle \varepsilon^{m/2} \rangle}{\langle \varepsilon \rangle^{m/2}} \left( \frac{r}{\eta} \right)^m, \tag{3.13}$$

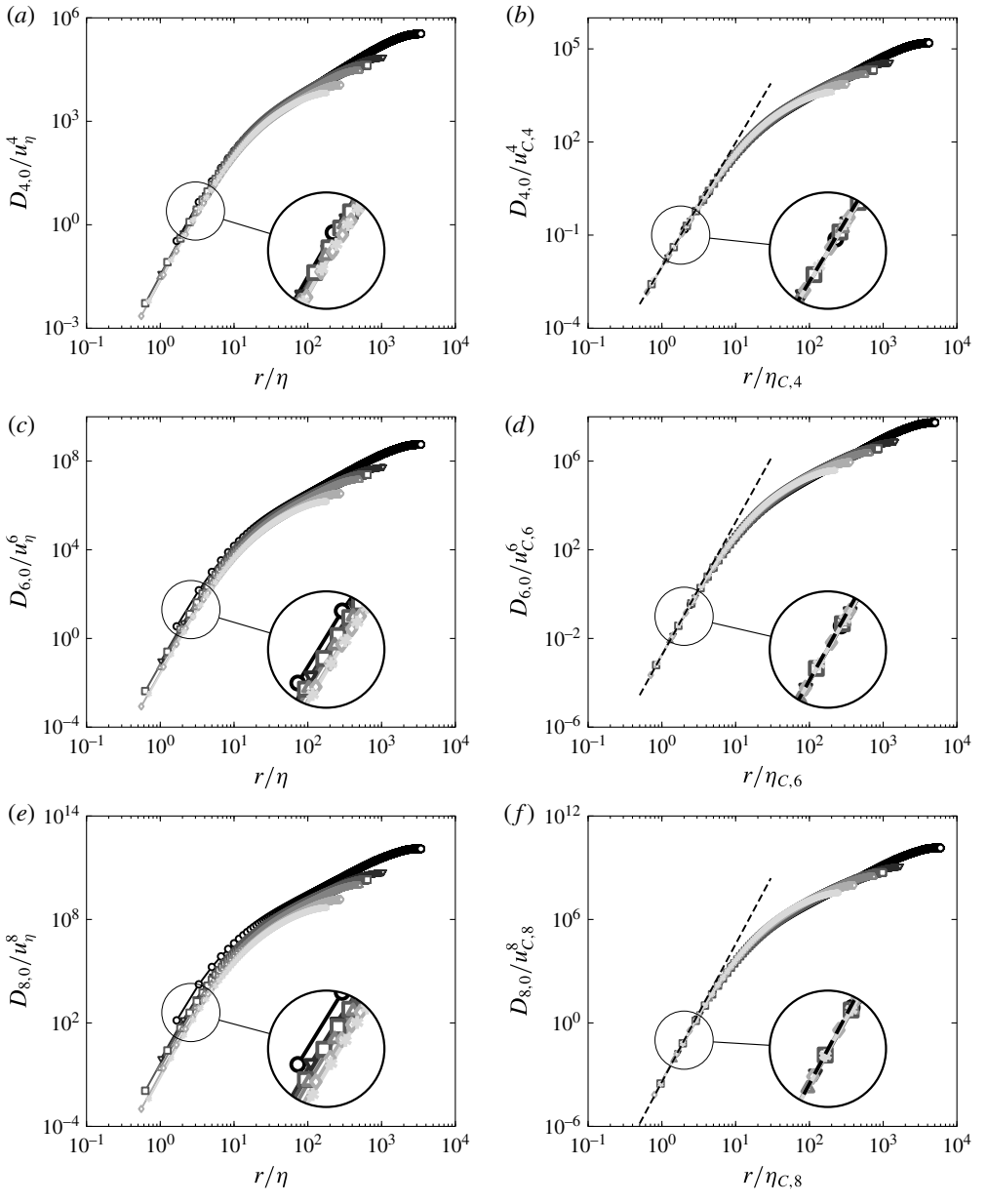


FIGURE 2. Longitudinal structure functions $D_{m,0}$: (*a*,*b*) $D_{4,0}$, (*c*,*d*) $D_{6,0}$, and (*e*,*f*) $D_{8,0}$. (*a*,*c*,*e*) Kolmogorov scaling with $\eta$ and $u_\eta$. (*b*,*d*,*f*) Scaling with $\eta_C$ (3.14) and $u_C$ (3.15). Symbols: $*$, $Re_\lambda = 88$; $\diamond$, $Re_\lambda = 119$; $\triangle$, $Re_\lambda = 184$; $\square$, $Re_\lambda = 215$; $\triangledown$, $Re_\lambda = 331$; and $\bigcirc$, $Re_\lambda = 754$. Dashed lines correspond to (3.16) with $\widetilde{K}_{4,0} = 1/105$ (*b*), $\widetilde{K}_{6,0} = 1/567$ (*d*) and $\widetilde{K}_{8,0} = 1/2673$ (*f*).

where the Reynolds-number dependence of $\langle\varepsilon^{m/2}\rangle/\langle\varepsilon\rangle^{m/2}$ increases with increasing order $m$. Consequently, Kolmogorov scaling cannot collapse structure functions different from those at the second order ($m = 2$) in the dissipative range, as is clearly

seen in the left column of figure 2. By introducing a modified order-dependent cut-off length scale,

$$\eta_{C,m} = \left( \frac{\nu^3}{\langle \varepsilon^{m/2} \rangle^{2/m}} \right)^{1/4}, \tag{3.14}$$

and a cut-off velocity,

$$u_{C,m} = (\nu \langle \varepsilon^{m/2} \rangle^{2/m})^{1/4}, \tag{3.15}$$

we find (3.9) normalised as

$$\frac{D_{m,0}}{u_{C,m}^m} = \widetilde{K}_{m,0} \left( \frac{r}{\eta_{C,m}} \right)^m, \tag{3.16}$$

in the spirit of Kolmogorov's 1941 work on the dissipative range for the second order, where the prefactor is constant. This scaling is shown in the right column of figure 2, again for $D_{4,0}$, $D_{6,0}$ and $D_{8,0}$ for different Reynolds numbers. Thus, (3.16) indeed collapses the structure functions for $r \to 0$, and $\widetilde{K}_{m,0}$ is universal in the sense that it does not depend on the Reynolds number but is an order-dependent constant with the exact values $\widetilde{K}_{2,0} = 1/15$, $\widetilde{K}_{4,0} = 1/105$ and so on. This collapse also serves as a numerical confirmation of the relation between the moments of the dissipation and the even moments of the longitudinal velocity gradient as reported by Boschung (2015). We find (3.16) to hold for $r = 0$ to $r/\eta_{C,m} \approx 10$ independent of the order. That is, the order-dependent dissipation range scales with $\eta_{C,m}$ as expected. As seen in figure 2, this clearly holds for even orders in general, due to (3.9). We note in passing that

$$Re_{C,m} = \frac{u_{C,m}\eta_{C,m}}{\nu} = 1, \tag{3.17}$$

as we might have expected, i.e. that inertial and viscous forces balance. Consequently, $\eta_{C,m}$ and $u_{C,m}$ are indeed viscous scales; for order $m = 2$, K41 scaling (i.e. the classical Kolmogorov scaling) is recovered, as $\eta_{C,2} = \eta$ and $u_{C,2} = u_\eta$.

Let us look at the cut-off length from a slightly different point of view. Considering only the longitudinal even-ordered structure functions, which are determined by the velocity gradients $\langle (\partial u_1/\partial x_1)^m \rangle$ with dimensional units $[\mathrm{s}^{-m}]$, one needs a second quantity with dimensions $[\mathrm{m}^\alpha\ \mathrm{s}^\beta]$ (with $\alpha \neq 0$ and $\beta \neq 0$) to find a characteristic length scale $l_m$ with dimensional units [m]. As we are concerned with the dissipative range, the viscosity $\nu$ with dimensions $[\mathrm{m}^2\ \mathrm{s}^{-1}]$ is a natural choice. We then have

$$\begin{aligned} l_m = \left[ \frac{\nu^m}{\langle (\partial u_1/\partial x_1)^m \rangle} \right]^{1/(2m)} &= \left[ \frac{\nu^{(3/2)m}}{\nu^{m/2} \langle (\partial u_1/\partial x_1)^m \rangle} \right]^{1/(2m)} \\ &\sim \left[ \frac{\nu^3}{\langle \varepsilon^{m/2} \rangle^{2/m}} \right]^{1/4} = \eta_{C,m} \end{aligned} \tag{3.18}$$

and similarly for $u_{C,m}$. That is, when choosing the viscosity as the second quantity to build the length scale, $\eta_{C,m}$ and $u_{C,m}$ naturally follow. Different scales can only be obtained by choosing a different quantity than $\nu$.

Different from the dissipative range, it is not possible to determine *a priori* how to normalise $D_{m,0} = C_{m,0} r^{\zeta_m}$ in the inertial range so that $C_{m,0}$ does not depend on

the Reynolds number. This is due to the fact that we do not know the exact value of $\zeta_m$ and thus cannot choose suitable velocity and length scales so that $C_m$ is non-dimensional; therefore we cannot expect the structure functions to collapse in the inertial range. The only exception is of course the third-order structure function $D_{3,0} = -(4/5)\langle\varepsilon\rangle r$, which collapses using the K41 scales $u_\eta$ and $\eta$. Deviations from K41 for the second-order structure functions in the inertial range are usually attributed to intermittency effects. For higher orders, it is therefore necessary to consider deviations of the higher-order structure functions normalised in such a way that they collapse for $r \to 0$ (as do the second-order structure functions when normalised with the K41 quantities), i.e. not with $\eta$ and $u_\eta$ but with $\eta_{C,m}$ (3.14) and $u_{C,m}$ (3.15). If one examines deviations of higher-order structure functions normalised with the second-order quantities $\eta$ and $u_\eta$, one includes the well-known increase of higher-order derivative moments scaled by the second moment. These effects are not present when using $\eta_{C,m}$ and $u_{C,m}$, as with these scales the Reynolds-number dependence cancels out.

Next, we also look at the odd orders, which should be determined by $\langle\omega_i S_{ij}\omega_j\rangle$ (third order), $\langle\omega_i S_{ij}S_{ik}S_{kl}\omega_l\rangle$ (fifth order) and so on. We find that their behaviour resembles that of the even orders, inasmuch as Kolmogorov scaling (3.3) does not collapse the structure functions for $r \to 0$ (cf. the left column of figure 3). Again, we find that deviations increase with increasing order and Reynolds number, as was the case for the even orders. Using $\eta_{C,m}$ (3.14) and $u_{C,m}$ (3.15) collapses the data and again we have an order-dependent dissipation range up to $r/\eta_{C,m} \sim 10$. Thus, the general relation (3.16) also holds for odd orders, although we cannot determine the prefactors $\widetilde{K}_{m,0}$ analytically. Furthermore, we would expect the odd moments of the (longitudinal) velocity gradient probability density function (p.d.f.) to scale with $\langle\varepsilon^{m/2}\rangle/\langle\varepsilon\rangle^{m/2}$, if $\langle(\partial u_1/\partial x_1)^m\rangle \sim \nu^{m/2}\langle\varepsilon^{m/2}\rangle$ for odd orders as well, as our data suggest. Ishihara *et al.* (2007) find $0.11 \pm 0.1$ for the Reynolds-number dependence of the skewness of $\partial u_1/\partial x_1$, which agrees with the scaling $\langle\varepsilon^{3/2}\rangle/\langle\varepsilon\rangle^{3/2} \sim Re_\lambda^{0.12}$ from our DNS. This implies that $\langle\varepsilon^{3/2}\rangle \sim \nu^{3/2}\langle\omega_i S_{ij}\omega_j\rangle$ and so on, with constant proportionality factors. However, these factors cannot be determined by the isotropic form of the general velocity gradient tensor, as $\langle\varepsilon^{3/2}\rangle$ etc. cannot be expressed in terms of it.

To summarise, $\eta_{C,m}$ and $u_{C,m}$ are the right quantities to non-dimensionalise structure functions in the dissipative range, as shown in figures 2 and 3. Using the new scales $\eta_{C,m}$ and $u_{C,m}$ collapses the higher orders as well as $\eta$ and $u_\eta$ in the case of the second order (cf. figure 1).

Naturally, the question arises how $\eta_{C,m}$ scales with $\eta$. From (3.14) we find

$$\frac{\eta_{C,m}}{\eta} = \left(\frac{\langle\varepsilon\rangle^{m/2}}{\langle\varepsilon^{m/2}\rangle}\right)^{1/(2m)} \sim Re_\lambda^{-\alpha_{m/2}/(2m)}. \tag{3.19}$$

Figure 4 shows the scaling of $\langle\varepsilon^{m/2}\rangle/\langle\varepsilon\rangle^{m/2}$ as a function of the Reynolds number $Re_\lambda$ as evaluated from our DNS,

$$\frac{\langle\varepsilon^{m/2}\rangle}{\langle\varepsilon\rangle^{m/2}} \sim Re_\lambda^{\alpha_{m/2}}, \tag{3.20}$$

where the dashed lines correspond to a least-squares fit and we use the values of $\alpha_{m/2}$ from our DNS in the following. Noticeably, the scaling exponent $\alpha_{m/2}$ of (3.20) increases with $m$, in agreement with the notion of intermittency of $\varepsilon$. Donzis, Yeung & Sreenivasan (2008) compared $\langle\varepsilon^{m/2}\rangle$ and $\langle\varepsilon\rangle^{m/2}$ as well as the ratio for different orders

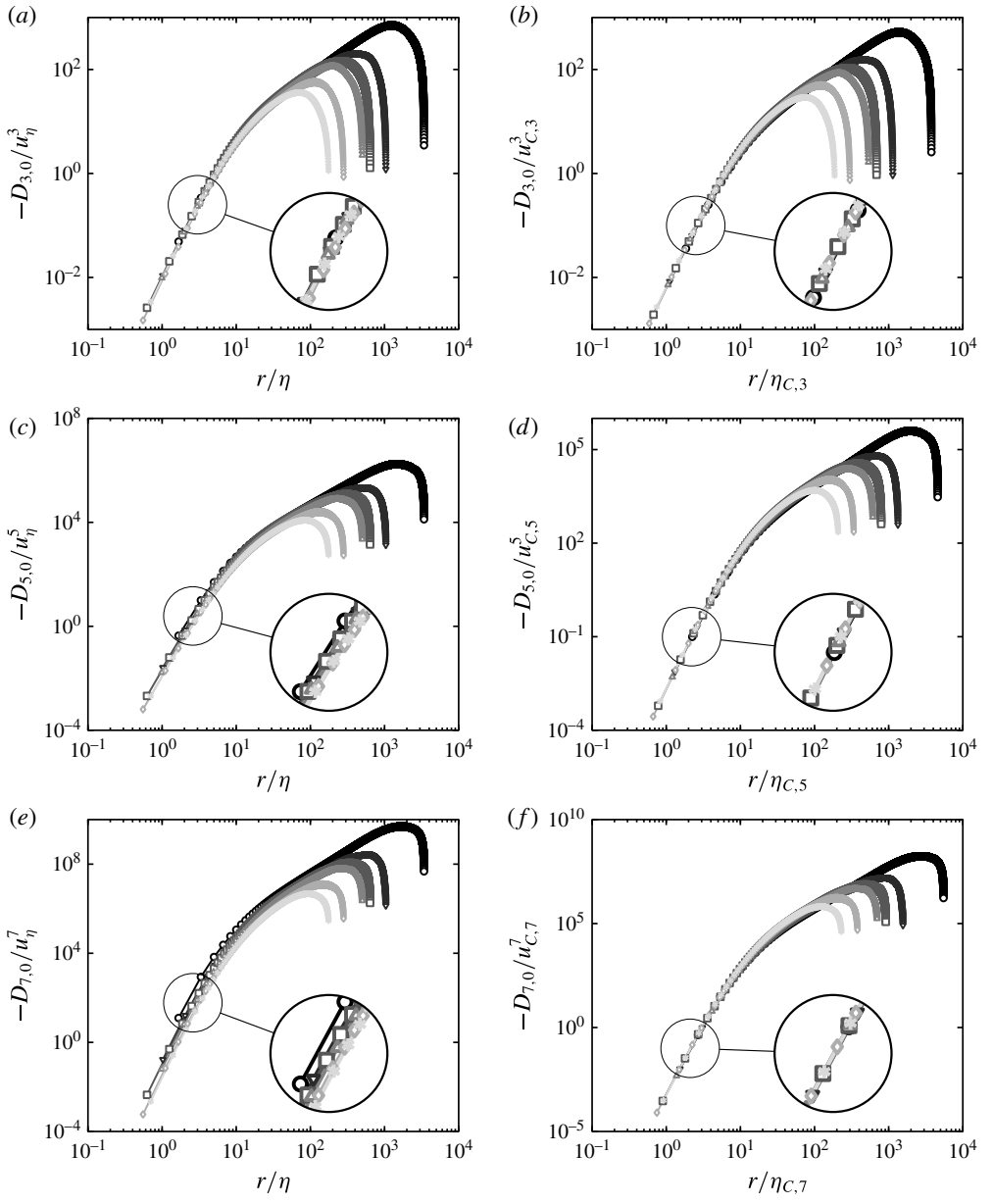


FIGURE 3. Longitudinal structure functions $D_{m,0}$: (*a*,*b*) $D_{3,0}$, (*c*,*d*) $D_{5,0}$, and (*e*,*f*) $D_{7,0}$. (*a*,*c*,*e*) Kolmogorov scaling with $\eta$ and $u_\eta$. (*b*,*d*,*f*) Scaling with $\eta_C$ (3.14) and $u_C$ (3.15). Symbols: $*$, $Re_\lambda = 88$; $\diamond$, $Re_\lambda = 119$; $\triangle$, $Re_\lambda = 184$; $\square$, $Re_\lambda = 215$; $\triangledown$, $Re_\lambda = 331$; and $\bigcirc$, $Re_\lambda = 754$.

$m/2 = 2, 3, 4$ as a function of the Reynolds number and grid resolution. They find that a grid resolution $\kappa_{max}\eta$ somewhere between $\kappa_{max}\eta = 1$ and $\kappa_{max}\eta = 3$ is sufficient to resolve the second to fourth moments of $\varepsilon$. Interestingly enough, the sensitivity of the normalised moments with respect to the resolution $\kappa_{max}\eta$ seems to decrease with increasing Reynolds number, at least for the two cases $Re_\lambda = 140$ and $Re_\lambda = 240$ that

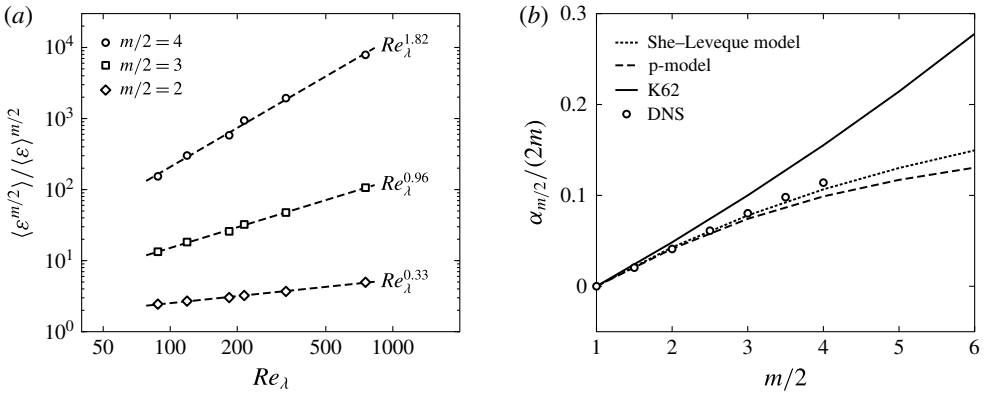


FIGURE 4. (*a*) Scaling of $\langle \varepsilon^{m/2} \rangle / \langle \varepsilon \rangle^{m/2}$ as a function of the Reynolds number. (*b*) Plot of $\alpha_{m/2}/(2m)$ as a function of $m/2$. Symbols, DNS data; solid line, K62 theory with $\mu = 0.25$; dashed line, p-model with $p_1 = 0.7$; dotted line, She–Leveque model.

they considered (their figure 4 and table 2). For that matter, we feel rather confident that the data shown in our figure 4(*a*,*b*) are adequate for the issues addressed in the present study, although we cannot claim that there might be no (small) errors in the values of $\alpha_{m/2}$ used below. In a recent paper, Schumacher *et al.* (2014) compared different flows for $m/2 = 2, 3, 4$ and found that the Reynolds-number dependence of $\langle \varepsilon^{m/2} \rangle / \langle \varepsilon \rangle^{m/2}$ is the same for the different flows they examined (homogeneous isotropic turbulence, a turbulent channel flow and turbulent Rayleigh–Bénard convection). This implies that the moments of the (longitudinal) velocity gradient should also have the same Reynolds-number dependence for the different flow types. This seems to be the case; Sreenivasan & Antonia (1997) and Ishihara *et al.* (2007) compiled data of different flows and found a good collapse of the skewness and flatness of the longitudinal velocity gradient.

Thus, the cut-off length $\eta_{C,m}$ decreases with increasing Reynolds number $Re_\lambda$, while the order dependence needs to be examined more closely. Figure 4(*b*) shows the ratio $\alpha_{m/2}/(2m)$ for $m = 1, \ldots, 8$, where $\alpha_{m/2}$ has been obtained by fitting the data of figure 4(*a*). We find that $\alpha_{m/2}/(2m)$ plotted over $m/2$ is concave and non-decreasing, at least for the orders observed. This can also be seen in figure 2, where the transitional range is shifted towards smaller scales with increasing order. This immediately raises the question of the asymptotic behaviour of $\alpha_{m/2}$ at high orders, as it would imply that there is a myriad of smaller and smaller scales ($m/2$ is unbounded in principle). If there is no upper limit of $\alpha$ for $m \to \infty$, then the smallest scale $\eta_{m\to\infty} \to 0$ independent of the Reynolds number, as seen from (3.19).

## 4. Scaling of the normalised dissipation

With the definition of the scales $\eta_{C,m}$, it is natural to write

$$\frac{\langle \varepsilon^{m/2} \rangle}{\langle \varepsilon \rangle^{m/2}} \sim \frac{\langle \varepsilon_r^{m/2} \rangle}{\langle \varepsilon \rangle^{m/2}}\bigg|_{r\to\eta_{C,m}} \sim \left(\frac{\eta_{C,m}}{\eta}\right)^{\gamma_{m/2}} \left(\frac{\eta}{L}\right)^{\gamma_{m/2}}, \tag{4.1}$$

where $\varepsilon_r$ is the volume-averaged dissipation as proposed by Obukhov (1962) and where $\gamma_{m/2}$ is the scaling exponent of the normalised dissipation,

$$\frac{\langle \varepsilon_r^{m/2} \rangle}{\langle \varepsilon \rangle^{m/2}} \sim \left( \frac{r}{L} \right)^{\gamma_{m/2}}. \tag{4.2}$$

With (3.19) and (3.20), we then find with $\eta/L \sim Re_\lambda^{-3/2}$ that

$$\alpha_{m/2} = -\frac{3}{2} \left( \frac{\gamma_{m/2}}{1 + \gamma_{m/2}/(2m)} \right), \tag{4.3}$$

and consequently any model specifying $\gamma_{m/2}$ can be used to determine $\alpha_{m/2}$. If one assumes together with Kolmogorov (1962) the ansatz

$$D_{p,0} \sim \langle \varepsilon_r^{p/3} \rangle r^{p/3} \sim r^{\zeta_p}, \tag{4.4}$$

as is widely accepted, also $\gamma_{m/2} = \zeta_{3(m/2)} - m/2$, and therefore any theory predicting the structure function scaling exponents $\zeta_{3(m/2)}$ predicts $\alpha_{m/2}$. One could also look at $\alpha$ in a different way: given $\alpha$, e.g. by some theory or measurements, one can solve for $\gamma$ and then use $\gamma_{m/2} = \zeta_{3(m/2)} - m/2$ to compute the scaling exponents,

$$\zeta_{3(m/2)} = \frac{m}{2} \left( 1 - 4 \frac{\alpha_{m/2}}{\alpha_{m/2} + 3m} \right). \tag{4.5}$$

Then, the larger $\alpha_{m/2}$, the larger are the deviations from K41 scaling $\zeta_{3(m/2)} = m/2$ for a given $m$. As larger values of $\alpha_{m/2}$ imply larger higher moments of the dissipation, this is consonant with the notion that anomalous scaling is connected to the intermittency of the dissipation.

Since $\zeta_{3(m/2)} > 0$ for all $m$, we find from (4.5) an upper limit for the scaling of the normalised dissipation as well as the ratio of the order-dependent scales,

$$\alpha_{m/2} \leqslant m, \quad \frac{\alpha_{m/2}}{2m} \leqslant \frac{1}{2}. \tag{4.6a,b}$$

Because $\alpha_{m/2}$ increases with increasing $m/2$ and $\alpha_1 = 0$, this implies that $\alpha_{m/2}/(2m)$ is concave and that $\alpha_{m/2}/(2m)$ increases linearly for large $m$.

Let us now briefly look at some well-known theories found in the literature and compare their predictions with our DNS. For the rest of this section, we consider even $m$, i.e. $m/2 = 1, 2, 3, \ldots$.

K62 theory (Kolmogorov 1962) assumes a log-normal distribution for the dissipation, which gives

$$\alpha_{m/2,K62} = \frac{m}{2} \frac{6\mu(m/2 - 1)}{8 + \mu(1 - m/2)}, \tag{4.7}$$

where $\mu$ is a coefficient parametrising the intermittency. Sreenivasan & Kailasnath (1993) concluded that $\mu = 0.25 \pm 0.05$. From (4.7), $\alpha_{1,K62} = 0$ as required. However, K62 gives $\alpha_{m/2,K62} \to \infty$ for $m/2 \to 8/\mu + 1$ and negative $\alpha_{m/2,K62}$ for $m/2 > 8/\mu + 1$. Similarly, the ratio $\eta_{C,m}/\eta \to 0$ for $m/2 \to 8/\mu + 1$, while $\eta_{C,m} > \eta$ for $m/2 > 8/\mu + 1$. This is at odds with the observation that the normalised moments $\langle \varepsilon^{m/2} \rangle / \langle \varepsilon \rangle^{m/2}$ increase with increasing Reynolds number for $m/2 > 1$, i.e. $\alpha_{m/2} > 0$ for all $m/2 > 1$.

When using K62, at first the moments $\langle \varepsilon^{m/2} \rangle$ strongly increase with $Re_\lambda$ and then strongly decrease when $m/2$ is increased further. Similarly, the order-dependent scales $\eta_{C,m}$ become smaller and smaller than the Kolmogorov scale and then jump to $\eta_{C,m} > \eta$ after a critical threshold. With $\mu = 0.25$, we find the singularity for the 33rd moment of the normalised dissipation and a reduced intermittency for $m/2 > 33$.

Multi-fractality of the dissipation (4.2) has been examined in detail by Meneveau & Sreenivasan (1991). An example for such a multi-fractal model is, for example, the p-model (see Meneveau & Sreenivasan 1987), which assumes that an eddy breaks up into two smaller eddies receiving fractions $p_1$ and $p_2 = 1 - p_1$ of the energy. The p-model then yields

$$\alpha_{m/2,p} = 6\,\frac{m/2 - \{1 - \log_2[p_1^{m/2} + (1 - p_1^{m/2})]\}}{3 + (2/m)\{1 - \log_2[p_1^{m/2} + (1 - p_1^{m/2})]\}}. \tag{4.8}$$

The p-model then gives $\alpha_{1,p} = 0$, while for $m/2 \to \infty$, $\alpha_{m/2,p} \to m$ because the parameter $p_1 \leqslant 1$.

Different from the (multi-)fractal framework, She & Leveque (1994) proposed a hierarchy of powers of the dissipation moments $\epsilon_r^{m/2} = \langle \varepsilon_r^{m/2+1} \rangle / \langle \varepsilon^{m/2} \rangle$. They then assumed that $\epsilon_r^{m/2+1}$ is determined by $\epsilon_r^{m/2}$ and $\epsilon_r^{\infty}$ for all $m/2$. Dubrulle (1994) and She & Waymire (1995) found that the She–Leveque model corresponds to the assumption of a log-Poisson distribution for the dissipation. The She–Leveque model yields

$$\alpha_{m/2,SL} = 6\,\frac{m/2 - 3\left[1 - \left(\frac{2}{3}\right)^{m/2}\right]}{5 + \frac{3}{m/2}\left[1 - \left(\frac{2}{3}\right)^{m/2}\right]}, \tag{4.9}$$

which contains no parameters, different from the other models examined in this section. The She–Leveque model has been found to be in excellent agreement with structure function exponents obtained by measurements and DNS (see e.g. Anselmet *et al.* 1984; Benzi *et al.* 1995; Gotoh, Fukayama & Nakano 2002). Similarly to the other models examined here, the She–Leveque model gives $\alpha_{1,SL} = 0$ and, for $m/2 \to \infty$, $\alpha_{m/2,SL} \to (6/5)(m/2)$, i.e. for very large $m$, $\langle \varepsilon^{m/2} \rangle / \langle \varepsilon \rangle^{m/2}$ scales linearly. Therefore, the order-dependent cut-off scales $\eta_{C,m}/\eta$ scale as $\alpha_{m/2}/2m \to 3/10$ for large $m/2$ and the She–Leveque model satisfies (4.6), i.e. the cut-off scales remain bounded at finite Reynolds numbers.

The $\alpha_{m/2}$ as computed from the three models above are shown in figure 4(*b*). While K62 overpredicts $\alpha_{m/2}$ as expected, both the p-model and the She–Leveque model are in very good agreement with our DNS. Structure function exponents as computed with (4.5) using the $\alpha_{m/2}$ from our DNS are shown in table 2, together with the measurements of Anselmet *et al.* (1984) and Gotoh *et al.* (2002), which we have averaged when more than one value was reported. While we find very good agreement, it should be kept in mind that the higher orders (for both the measurements of Anselmet *et al.* (1984) and the DNS of Gotoh *et al.* (2002) as well as the ones computed from our data) might be subject to significant error bands. It is also worth mentioning that numerical errors in $\alpha_{m/2}$ translate to smaller errors in $\zeta_{3(m/2)}$, at least up to $m/2 = 4$. This error decreases with increasing $m/2$: for instance, $\alpha_2 \pm 10\,\%$ yields $\zeta_6 \pm 3.77\,\%$, while $\alpha_4 \pm 10\,\%$ yields $\zeta_{12} \pm 1.16\,\%$.

| $m/2$ | Equation (4.5) | Anselmet *et al.* (1984) | Gotoh *et al.* (2002) |
|---|---|---|---|
| 1 | $\zeta_3 = 1$ | $\zeta_3 = 1$ | $\zeta_3 = 1.015$ |
| 2 | $\zeta_6 = 1.7871$ | $\zeta_6 = 1.8$ | $\zeta_6 = 1.78$ |
| 3 | $\zeta_9 = 2.3904$ | $\zeta_9 = 2.465$ | $\zeta_9 = 2.35$ |
| 4 | $\zeta_{12} = 2.8696$ | $\zeta_{12} = 2.84$ | — |

TABLE 2. Comparison of $\zeta_{3(m/2)}$ computed with (4.5) using $\alpha_{m/2}$ from our DNS and literature.

## 5. Resolution requirements

From the existence of scales smaller than the Kolmogorov scale, it follows that this might influence the resolution requirements of DNS, as characterised by the product $\kappa_{max}\eta$, where $\kappa_{max}$ is the maximum wavenumber resolved by the simulation. Different from earlier work, e.g. by Yakhot & Sreenivasan (2005), where the multi-fractal model was used to determine the cut-off scales, we use here the exact length scales (3.14). It is therefore worthwhile to examine the required grid resolution in some detail, although it has been studied in the literature by employing different approaches before. Naturally, there is a trade-off for a given number of grid points corresponding to a given $\kappa_{max}$ between a highly resolved simulation (i.e. a large $\kappa_{max}\eta$) and a high Reynolds number implying a low $\kappa_{max}\eta$. Common wisdom is to resolve at least $k_{max}\eta = 1$ and usually $\kappa_{max}\eta = 1.3$ is considered high enough. Note that some studies require a higher resolution, especially if the examined quantities depend on high-order derivatives of the velocity field. An example is the study of Jiménez *et al.* (1993), which required $\kappa_{max}\eta = 2$.

It is evident that $\kappa_{max}\eta > 1$ is needed to resolve the higher moments of the velocity gradient p.d.f., as these are linked to the higher moments of the dissipation. The higher the order of the moment, the higher the necessary resolution. This can also be seen from the data of Ishihara *et al.* (2007) as well as Donzis *et al.* (2008), where the velocity gradient p.d.f. did not collapse at similar Reynolds number with $\kappa_{max}\eta = 1$ and $\kappa_{max}\eta = 2$; the dissimilarity is less in the core of the p.d.f. and stronger in the tails, which are determined by the higher moments.

From (3.19), we see that the cut-off lengths $\eta_{C,m}$ are less resolved for a given $\kappa_{max}\eta$ with increasing order $m$. In order to compare these influences, the normalised resolution

$$[\kappa_{max}\eta_{C,m}]^* = \frac{\kappa_{max}\eta_{C,m}}{\kappa_{max}\eta} \tag{5.1}$$

is provided in table 3, where we have used the values of $\langle\varepsilon^{m/2}\rangle/\langle\varepsilon\rangle^{m/2}$ from our data. We also give extrapolated resolutions for $Re_\lambda = 10^3$ and $Re_\lambda = 10^4$, which were computed using the fits shown in figure 4(*a*). These resolutions are not meant to give exactly the required resolution to resolve the eighth order at $Re_\lambda = 10^3$, say, but rather to provide an estimate and to show the influence of the Reynolds number and order. For instance, $\kappa_{max}\eta = 1.3$ would suggest that the fourth-order structure function (and with it the flatness of the velocity gradient p.d.f.) is completely resolved at $Re_\lambda = 10^4$, while higher orders are only partially resolved. Equivalently, we would expect $\kappa_{max}\eta = 1.3$ at $Re_\lambda = 215$ to fully resolve the sixth-order structure function, i.e. this rule of thumb ensures a well enough resolved DNS, if one is interested in lower-order moments at (from the present point of view) low to intermediate Reynolds numbers.

| | R0 | R1 | R2 | R3 | R4 | R5 | $Re_\lambda = 10^3$ | $Re_\lambda = 10^4$ |
|---|---|---|---|---|---|---|---|---|
| $[\kappa_{max}\eta]^*$ | 1.000 | 1.000 | 1.000 | 1.000 | 1.000 | 1.000 | 1.000 | 1.000 |
| $[\kappa_{max}\eta_{C,4}]^*$ | 0.894 | 0.883 | 0.871 | 0.864 | 0.849 | 0.819 | 0.805 | 0.738 |
| $[\kappa_{max}\eta_{C,6}]^*$ | 0.806 | 0.785 | 0.763 | 0.749 | 0.725 | 0.678 | 0.663 | 0.551 |
| $[\kappa_{max}\eta_{C,8}]^*$ | 0.730 | 0.700 | 0.672 | 0.652 | 0.623 | 0.571 | 0.551 | 0.424 |

TABLE 3. Normalised resolution $[\kappa_{max}\eta_{C,m}]^* = \kappa_{max}\eta_{C,m}/\kappa_{max}\eta$ as a function of Reynolds number $Re_\lambda$ and order $m$.

To summarise, if $\kappa_{max}\eta = \kappa_{max}\eta_{C,2} = 1$ completely resolves the second-order structure function, the variance of the velocity gradient p.d.f., the mean dissipation $\langle\varepsilon\rangle$ and low-order statistics like the mean kinetic energy $\langle k\rangle$ (cf. Yeung & Pope 1989), then $\kappa_{max}\eta_{C,3} = 1$ additionally completely resolves the third-order structure function, the skewness of the velocity gradient p.d.f. and the vortex stretching $\langle\omega_i S_{ij}\omega_j\rangle$, while $\kappa_{max}\eta_{C,4} = 1$ also resolves the flatness of the velocity gradient p.d.f., the variance of the p.d.f. $P(\varepsilon)$ and the fourth-order structure function, and so on.

Thus, we need more grid points to resolve a certain order when increasing the Reynolds number than the classical estimate using K41 would suggest. There are several estimates of the scaling of numbers of grid points with the Reynolds number – see, for instance, Paladin & Vulpiani (1987*b*), Davidson (2004) and Yakhot & Sreenivasan (2005). In the following, we will use (3.19). If we assume that $\alpha_{m/2}/(2m)$ converges to a finite number for $m \to \infty$, we can use (3.19) to estimate the number of grid points to completely resolve all scales, sometimes also called the number of degrees of freedom of the flow. That is, we can estimate the scaling of grid points with the Reynolds number via

$$N \sim \left(\frac{L_{Box}}{\Delta x}\right)^3 \sim \left(\frac{L_{Box}}{L}\right)^3 \left(\frac{L}{\eta_{C,m\to\infty}}\right)^3 \sim \left(\frac{L_{Box}}{L}\right)^3 \left(\frac{L}{\eta}\right)^3 \left(\frac{\eta}{\eta_{C,m\to\infty}}\right)^3 \sim \left(\frac{L_{Box}}{L}\right)^3 Re_L^{9/4[1+\alpha_{m/2}/(3m)]}, \tag{5.2}$$

where $\Delta x$ is the grid spacing, $L_{Box}$ the length of the DNS box (cube) and $L$ the integral length. Consequently, $N$ is larger than the K41 estimate $N \sim Re_L^{9/4}$ since $\alpha_{m/2} \geqslant 0$ and the scaling of $N$ depends on the asymptotic behaviour of $\alpha_{m/2}/(2m)$ for $m/2 \to \infty$. From (4.6), $\alpha_{m/2}/(2m) \leqslant 1/2$ (i.e. $\alpha_{m/2}/(3m) \leqslant 1/3$) and therefore

$$N \sim \left(\frac{L_{Box}}{L}\right)^3 Re_L^3, \tag{5.3}$$

as upper bound. Paladin & Vulpiani (1987*b*) used the multi-fractal framework to also obtain $N \sim Re_L^3$ as the largest Reynolds-number scaling possible (see also Yakhot & Sreenivasan (2005), where also a $Re_L^3$ scaling has been found). For the She–Leveque model, $\alpha_{m/2}/(2m) \to 3/10$ and one obtains $N \sim Re_L^{27/10}$. Paladin & Vulpiani (1987*b*) reported $N \sim Re_L^{2.3}$ using data from Anselmet *et al.* (1984).

## 6. Conclusion

Let us briefly summarise the main results. Using relations between the moments of the longitudinal velocity gradient and the moments of the dissipation, we find

the exact solution of longitudinal structure functions in the dissipative range without ambiguity or any free parameters for arbitrary even orders as given by (3.9), where the $C_{m,0}$ are known universal (Reynolds-number-independent) constants. That is, we can precisely and without ambiguity show how the moments of the dissipation enter the structure function solutions in the dissipative range. The only required assumptions are (local) isotropy, (local) homogeneity and incompressibility. From this, we find generalised cut-off scales as given by (3.14) and (3.15). These scales are exact under the above assumptions and can be interpreted as a generalisation of the Kolmogorov scales $\eta$ and $u_\eta$ and are determined by dissipative quantities (the moments of the dissipation and the kinematic viscosity) only. The question then becomes whether the same results hold for mixed and transverse structure functions as well as odd orders. We find empirically from our data that this is indeed the case for the mixed and transverse structure functions, because the ratio of the velocity gradients $\langle(\partial u_2/\partial x_1)^{p+q}\rangle$ and $\langle(\partial u_1/\partial x_1)^p(\partial u_2/\partial x_1)^q\rangle$ to $\langle(\partial u_1/\partial x_1)^{p+q}\rangle$ is constant at sufficiently high Reynolds number, as was previously shown by Ishihara *et al.* (2007). However, these constants can only be determined numerically. Also, we find that using moments $\langle\varepsilon^{m/2}\rangle$ with odd $m$ collapses the odd-order structure functions, although the required connectors again cannot be derived. As the normalised moments of the dissipation increase with increasing Reynolds number and order, the cut-off length scales $\eta_{C,m}$ decrease. Again, we want to emphasise that we only employ the same assumptions as Kolmogorov in his 1941 papers (Kolmogorov 1941*a*,*b*) and the results of the present paper can be viewed as a generalisation of Kolmogorov's work for higher orders in the dissipative range. This implies that K41 scaling is only correct for the second order (and for the third order in the inertial range), while for higher orders the new scales should be used, which are defined by (3.14) and (3.15) without any ambiguity or additional assumptions. At scales $r \sim O(\eta_{C,m})$, the normalised moments of the dissipation cross over to the volume-averaged dissipation $\varepsilon_r$. Consequently, any theory predicting the scaling of $\varepsilon_r$ or the structure function exponents in the inertial range, $\zeta$, can be used to determine the scaling of $\eta_{C,m}$. We find that K62 makes unphysical predictions, while both the multi-fractal p-model as well as the She–Leveque model agree very well with our DNS. As there is a myriad of order-dependent (and Reynolds-number-dependent) cut-off length scales, the grid needs to be finer with increasing order and Reynolds number, an effect well known in the literature, which is not captured by K41. We use the exact cut-off lengths of § 5 and our DNS data to estimate the grid resolution at a given order, which gives satisfactory agreement with previous results in the literature. Thus when carrying out DNS studies, one should consider the desired Reynolds number that one is aiming at as well as the order that needs to be fully resolved. Resolving the (K41) Kolmogorov scale $\eta$ is sufficient to resolve the transport of kinetic energy down the cascade and its dissipation. Higher resolution is necessary if one is interested in higher-order statistics, which consequently need higher orders correctly resolved. This is evident inasmuch as the moments of the velocity gradient p.d.f. can be obtained from the limit of $D_{p,q}/r^{p+q}$ for $r \to 0$.

**Acknowledgements**

This work was supported by the Deutsche Forschungsgemeinschaft through the grant Pe 241/44-1 and benefited from many helpful discussions with Dr R. J. Hill. The authors gratefully acknowledge the computing time granted by the JARA-HPC-Vergabegremium provided on the JARA-HPC Partition part of the supercomputer JUQUEEN at the Forschungszentrum Jülich.

## REFERENCES


ANSELMET, F., GAGNE, Y. & HOPFINGER, E. 1984 High-order velocity structure functions in turbulent shear flows. *J. Fluid Mech.* **140** (63), 63–89.

BENZI, R., CILIBERTO, S., BAUDET, C. & CHAVARRIA, G. R. 1995 On the scaling of three-dimensional homogeneous and isotropic turbulence. *Physica* D **80** (4), 385–398.

BENZI, R., CILIBERTO, S., TRIPICCIONE, R., BAUDET, C., MASSAIOLI, F. & SUCCI, S. 1993 Extended self-similarity in turbulent flows. *Phys. Rev.* E **48** (1), R29–R32.

BETCHOV, R. 1956 An inequality concerning the production of vorticity in isotropic turbulence. *J. Fluid Mech.* **1** (05), 497–504.

BOSCHUNG, J. 2015 Exact relations between the moments of dissipation and longitudinal velocity derivatives in turbulent flows. *Phys. Rev.* E **92** (4), 043013.

DAVIDSON, P. A. 2004 *Turbulence: An Introduction for Scientists and Engineers*. Oxford University Press.

DONZIS, D., YEUNG, P. & SREENIVASAN, K. 2008 Dissipation and enstrophy in isotropic turbulence: resolution effects and scaling in direct numerical simulations. *Phys. Fluids* **20** (4), 045108.

DUBRULLE, B. 1994 Intermittency in fully developed turbulence: log-Poisson statistics and generalized scale covariance. *Phys. Rev. Lett.* **73** (7), 959–962.

ESWARAN, V. & POPE, S. 1988 Direct numerical simulations of the turbulent mixing of a passive scalar. *Phys. Fluids* **31**, 506–520.

FRISCH, U. 1995 *Turbulence: The Legacy of AN Kolmogorov*. Cambridge University Press.

FRISCH, U. & VERGASSOLA, M. 1991 A prediction of the multifractal model: the intermediate dissipation range. *Europhys. Lett.* **14**, 439–444.

GOTOH, T., FUKAYAMA, D. & NAKANO, T. 2002 Velocity field statistics in homogeneous steady turbulence obtained using a high-resolution direct numerical simulation. *Phys. Fluids* **14**, 1065.

HIERRO, J. & DOPAZO, C. 2003 Fourth-order statistical moments of the velocity gradient tensor in homogeneous, isotropic turbulence. *Phys. Fluids* **15** (11), 3434–3442.

HILL, R. J. 2001 Equations relating structure functions of all orders. *J. Fluid Mech.* **434** (1), 379–388.

HOU, T. Y. & LI, R. 2007 Computing nearly singular solutions using pseudo-spectral methods. *J. Comput. Phys.* **226** (1), 379–397.

ISHIHARA, T., KANEDA, Y., YOKOKAWA, M., ITAKURA, K. & UNO, A. 2007 Small-scale statistics in high-resolution direct numerical simulation of turbulence: Reynolds number dependence of one-point velocity gradient statistics. *J. Fluid Mech.* **592**, 335–366.

JIMÉNEZ, J., WRAY, A., SAFFMAN, P. & ROGALLO, R. 1993 The structure of intense vorticity in isotropic turbulence. *J. Fluid Mech.* **255**, 65–90.

DE KARMAN, T. & HOWARTH, L. 1938 On the statistical theory of isotropic turbulence. *Proc. R. Soc. Lond.* A **164** (917), 192–215.

KOLMOGOROV, A. N. 1941*a* Dissipation of energy in locally isotropic turbulence. *Dokl. Akad. Nauk. SSSR* **32**, 16–18.

KOLMOGOROV, A. N. 1941*b* The local structure of turbulence in incompressible viscous fluid for very large Reynolds numbers. *Dokl. Akad. Nauk. SSSR* **30**, 299–303.

KOLMOGOROV, A. N. 1962 A refinement of previous hypotheses concerning the local structure of turbulence in a viscous incompressible fluid at high Reynolds number. *J. Fluid Mech.* **13** (1), 82–85.

LANDAU, L. D. & LIFSHITZ, E. M. 1959 *Fluid Mechanics*, Course of Theoretical Physics, vol. 6. Pergamon.

LI, N. & LAIZET, S. 2010 2DECOMP and FFT – a highly scalable 2D decomposition library and FFT interface. In *Cray User Group 2010 Conference*, pp. 1–13.

MENEVEAU, C. 1996 Transition between viscous and inertial-range scaling of turbulence structure functions. *Phys. Rev.* E **54** (4), 3657.

MENEVEAU, C. & SREENIVASAN, K. 1987 Simple multifractal cascade model for fully developed turbulence. *Phys. Rev. Lett.* **59** (13), 1424.

MENEVEAU, C. & SREENIVASAN, K. 1991 The multifractal nature of turbulent energy dissipation. *J. Fluid Mech.* **224** (429–484), 180.

OBUKHOV, A. R. 1962 Some specific features of atmospheric turbulence. *J. Fluid Mech.* **13**, 77–81.

PALADIN, G. & VULPIANI, A. 1987*a* Anomalous scaling laws in multifractal objects. *Phys. Rep.* **156** (4), 147–225.

PALADIN, G. & VULPIANI, A. 1987*b* Degrees of freedom of turbulence. *Phys. Rev.* A **35** (4), 1971.

POPE, S. B. 2000 *Turbulent Flows*. Cambridge University Press.

ROTTA, J. C. 1972 *Turbulente Strömungen,* vol. 8. B. G. Teubner.

SCHUMACHER, J., SCHEEL, J. D., KRASNOV, D., DONZIS, D. A., YAKHOT, V. & SREENIVASAN, K. R. 2014 Small-scale universality in fluid turbulence. *Proc. Natl Acad. Sci. USA* **111** (30), 10961–10965.

SCHUMACHER, J., SREENIVASAN, K. R. & YAKHOT, V. 2007 Asymptotic exponents from low-Reynolds-number flows. *New J. Phys.* **9** (4), 89.

SHE, Z.-S. & LEVEQUE, E. 1994 Universal scaling laws in fully developed turbulence. *Phys. Rev. Lett.* **72** (3), 336.

SHE, Z.-S. & WAYMIRE, E. C. 1995 Quantized energy cascade and log-Poisson statistics in fully developed turbulence. *Phys. Rev. Lett.* **74** (2), 262.

SIGGIA, E. D. 1981 Invariants for the one-point vorticity and strain rate correlation functions. *Phys. Fluids* **24** (11), 1934–1936.

SREENIVASAN, K. 1991 Fractals and multifractals in fluid turbulence. *Annu. Rev. Fluid Mech.* **23** (1), 539–604.

SREENIVASAN, K. & ANTONIA, R. 1997 The phenomenology of small-scale turbulence. *Annu. Rev. Fluid Mech.* **29** (1), 435–472.

SREENIVASAN, K. & KAILASNATH, P. 1993 An update on the intermittency exponent in turbulence. *Phys. Fluids* A **5** (2), 512–514.

TOWNSEND, A. 1951 On the fine-scale structure of turbulence. *Proc. R. Soc. Lond.* A **208** (1095), 534–542.

YAKHOT, V. 2001 Mean-field approximation and a small parameter in turbulence theory. *Phys. Rev.* E **63** (2), 026307.

YAKHOT, V. 2003 Pressure–velocity correlations and scaling exponents in turbulence. *J. Fluid Mech.* **495**, 135–143.

YAKHOT, V. & SREENIVASAN, K. R. 2005 Anomalous scaling of structure functions and dynamic constraints on turbulence simulations. *J. Stat. Phys.* **121** (5–6), 823–841.

YEUNG, P. & POPE, S. 1989 Lagrangian statistics from direct numerical simulations of isotropic turbulence. *J. Fluid Mech.* **207** (1), 531–586.